

Holocene vegetation and biomass changes on the Tibetan Plateau

A. Dallmeyer et al.

Holocene vegetation and biomass changes on the Tibetan Plateau – a model-pollen data comparison

A. Dallmeyer¹, M. Claussen^{1,2}, U. Herzschuh³, and N. Fischer^{1,4}

¹Max Planck Institute for Meteorology, KlimaCampus Hamburg, Germany

²Meteorological Institute, University of Hamburg, KlimaCampus Hamburg, Germany

³Alfred Wegener Institute for Polar and Marine Research, Potsdam, Germany

⁴International Max-Planck-Research School, Hamburg, Germany

Received: 17 February 2011 – Accepted: 20 March 2011 – Published: 31 March 2011

Correspondence to: A. Dallmeyer (anne.dallmeyer@zmaw.de)

Published by Copernicus Publications on behalf of the European Geosciences Union.

Title Page

Abstract

Introduction

Conclusions

References

Tables

Figures

⏪

⏩

◀

▶

Back

Close

Full Screen / Esc

Printer-friendly Version

Interactive Discussion

Abstract

Results of a transient numerical experiment, performed in a coupled atmosphere-ocean-vegetation model with orbital forcing alone, are compared to pollen-based vegetation reconstructions from four representative sites on the Tibetan Plateau, covering the last 6000 years. Causes of the vegetation change and consequences for the biomass storage are analysed.

In general, simulated and reconstructed vegetation trends at each site are in good agreement. Both methods reveal a general retreat of the biomass-rich vegetation that is particularly manifested in a strong decrease of forests. However, model and reconstructions differ with regard to the climatic factors causing this vegetation change. The reconstructions primarily identify decreasing summer monsoon precipitation as the responsible mechanism for the vegetation shift. In the model, the land cover change originates from differences in near-surface air temperature arising out of orbitally-induced insolation changes.

According to the model results, the averaged forest fraction on the Plateau is shrinking by almost one-third from mid-Holocene (41.4%) to present-day (28.3%). Shrubs, whose fraction is quadrupled at present-day (12.3%), replace most of this forest. Gras fraction increases from 38.9% during the mid-Holocene to 42.3% at present-day. This land cover change results in a decrease of living biomass by 0.62 kgC m⁻². Total biomass on the Tibetan Plateau decreases by 1.9 kgC m⁻², i.e. approx. 6.64 PgC are released due to the natural land cover change.

1 Introduction

The Tibetan Plateau covers a region of approx. 2.5 million km². With an average height of more than 4000 m above sea level (a.s.l.), it penetrates deep into the troposphere reaching atmospheric levels of less than 500 hPa. Due to its large horizontal and vertical extent, the Tibetan Plateau affects the regional as well as the global climate,

CPD

7, 1073–1111, 2011

Holocene vegetation and biomass changes on the Tibetan Plateau

A. Dallmeyer et al.

Title Page

Abstract

Introduction

Conclusions

References

Tables

Figures

⏪

⏩

◀

▶

Back

Close

Full Screen / Esc

Printer-friendly Version

Interactive Discussion



Holocene vegetation and biomass changes on the Tibetan Plateau

A. Dallmeyer et al.

Title Page

Abstract

Introduction

Conclusions

References

Tables

Figures

⏪

⏩

◀

▶

Back

Close

Full Screen / Esc

Printer-friendly Version

Interactive Discussion



including the circulation, energy and water cycle (Wu et al., 2007). Besides the mechanical blocking of zonal as well as meridional atmospheric flow (e.g. Wu et al., 2005; Y. Liu et al., 2007), thermal processes on the Tibetan Plateau strongly influence the regional circulation. Acting as a heat source for the atmosphere in spring and summer the Tibetan Plateau plays an important role for the onset and maintenance of the Asian summer monsoon (e.g. Wu and Zhang, 1998; Ye and Wu, 1998; Wu, 2004; Y. Liu et al., 2007).

The large amount of air pumped up in the atmosphere above the Tibetan Plateau due to high convective activity diverges near the tropopause and subsides in the surroundings, forcing and forming dry climate and deserts in North Africa, Central Asia (e.g. Takla Makan, Dzungaria Desert) and in the Middle-East (Rodwell and Hoskins, 1996; Ye and Wu, 1998; Duan and Wu, 2005).

Recent studies proposed a strong relationship between the heating on the Plateau and the summer monsoon rainfall in East Asia (e.g. Hsu and Liu, 2003; Yanai and Wu, 2006; Zhang et al., 2006; Wang et al., 2008). Investigations based on observations as well as climate model sensitivity experiments suggest an enhancement of the moisture transport towards East Asia and increasing precipitation in the subtropical front (Mei-Yu, Baiu and Changma) in years with higher surface temperature on the Tibetan Plateau (Wang et al., 2008).

High-elevation snow accumulation is another important factor by which the Tibetan Plateau exerts influence on the Asian climate. Above-normal snow cover in winter weakens the land-sea temperature gradient and attenuates the East Asian monsoon in the subsequent summer (Y. Liu et al., 2007).

All these processes depend to a large part on the land cover of the Tibetan Plateau as it modulates the energy balance and the energy transfer between the atmosphere and the land surface (Yasunari, 2007). The albedo of the surface determines the absorbed incoming solar radiation and therewith the strength of diabatic heat fluxes. Changes in the Tibetan Plateau's land cover may thus exert strong influence on the regional and even on the northern hemispheric climate and atmospheric

Holocene vegetation and biomass changes on the Tibetan Plateau

A. Dallmeyer et al.

Title Page

Abstract

Introduction

Conclusions

References

Tables

Figures

⏪

⏩

◀

▶

Back

Close

Full Screen / Esc

Printer-friendly Version

Interactive Discussion



circulation. Beside the biogeophysical effects of changing albedo, surface roughness and evapotranspiration, land cover changes affect the climate via biogeochemical feedbacks, for example by the emission of carbon into the atmosphere (Claussen et al., 2001). Therefore, it is necessary to get more information about land cover changes on the Tibetan Plateau to understand past climate change in Asia.

So far, reconstructions suggest an increased mid-Holocene forest fraction on the eastern and southern margin of the Plateau compared to the present conditions (Shen et al., 2005, 2006). Enlarged monsoon rainfall and higher summer temperatures due to orbitally-induced insolation changes are seen as the most important forcing mechanisms for the vegetation change (Herzschuh et al., 2010b), but human impact is discussed as an influencing factor as well (Schlütz and Lehmkuhl, 2009). For the central Tibetan Plateau, reconstructions reveal only slight changes in vegetation composition during the Holocene (Tang et al., 2009). Fewer records are available for the western Tibetan Plateau. They indicate wetter climate conditions (Gasse et al., 1991) and more vegetation for the mid-Holocene. As pollen reconstructions can only illustrate the local vegetation distribution and can only be taken as proxies for climate change, it is important to perform model simulations to identify the mechanism behind the changes. Furthermore, Earth System Models (ESM) have the advantage of calculating area-wide vegetation and climate changes, taking feedback mechanisms into account. Thereby, it is possible to extract the driving parameters, regarding the Holocene climate and vegetation change on the Tibetan Plateau and surrounding monsoonal areas; even more, related changes in the terrestrial carbon storage can be quantified.

Since computing power is limited, long transient experiments in comprehensive Earth system models can only be performed with coarse numerical resolutions. Such an experiment has been conducted by Fischer et al. (2011) with the model ECHAM5/JSBACH-MPIOM, covering the last 6000 years.

The primary aim of this study is to critically assess the performance of that model with respect to the land cover on the Tibetan Plateau. For this purpose, we compare

pollen-based vegetation reconstructions for different sites on the Plateau with the simulated vegetation trend in the surrounding areas. Secondly, we want to identify the specific climatic parameters that caused the past vegetation changes. Thirdly, we quantify the total changes of vegetation carbon storage for the entire Tibetan Plateau.

2 Study area

2.1 The Tibetan Plateau

The Tibetan Plateau covers almost one-sixth of the area in China. Located in a tectonically active region (ca. 80–105° E and 27–37° N), the Plateau exhibits a highly complex orography with steep and huge mountain ranges as well as large elevated plains. The Tibetan Plateau penetrates deep into the troposphere. Thus, it shows unique climate conditions with the lowest surface temperature and pressure as well as highest 10-m wind speed compared to areas in the same latitudinal belt (Asnani, 1993).

The climate on the Tibetan Plateau is strongly determined by the Asian monsoon circulation (Fig. 1a). Summer monsoon precipitation provides more than 60% of the annual total (Cui and Graf, 2009). Additionally, the complex terrain affects climate and vegetation distribution. Following the general decrease in altitude, near-surface air temperature and precipitation increase from the north-western to the south-eastern part of the Plateau. In summer, the Plateau is characterised by near-surface temperatures up to 19 °C in the south-east and ca. 6 °C in the north-west (Sun, 1999). Winter temperatures are around 5–10 °C in the south-east and –25 °C in the north-west (Cui and Graf, 2009). Due to the strong insolation during daytime, near-surface air temperatures experience strong diurnal variations. Surface soil temperature varies up to 50 °C (spring) between day and night (Cui and Graf, 2009). Annual precipitation amounts are generally small on the Tibetan Plateau, reaching values of approximately

Holocene vegetation and biomass changes on the Tibetan Plateau

A. Dallmeyer et al.

Title Page

Abstract

Introduction

Conclusions

References

Tables

Figures

⏪

⏩

◀

▶

Back

Close

Full Screen / Esc

Printer-friendly Version

Interactive Discussion



700 mm in the south-eastern part and less than 100 mm in the north-western part (Sun, 1999). But precipitation strongly varies in time and space (Ueno et al., 2001).

The diverse climate conditions lead to a unique land cover on the Plateau. Strong temperature and precipitation gradients along the steep mountains offer a very heterogeneous environment for vegetation, but make the located vegetation also highly susceptible to climate change.

The spatial distribution of major vegetation types is described in the Vegetation Atlas of China (Hou, 2001) and summarised in Fig. 1b. Present-day vegetation along the wet and warm south-eastern and eastern margins of the Tibetan Plateau is dominated by montane conifer and broad-leaved forests, although intensive logging strongly reduced the forest extent. Above the treeline (ca. 3000–4000 m), sub-alpine shrubs cover the area, replaced by alpine and high-alpine meadows at higher elevations. The dry north-eastern and central Tibetan Plateau is characterised by temperate and alpine steppe vegetation. Alpine deserts form the landscape at the dry north-central and western Plateau.

2.2 Study sites for pollen-based vegetation reconstructions

In this study, pollen records from four different lakes are considered, representing different climate and vegetation zones on the Tibetan Plateau (see Fig. 1). These are Lake Qinghai and Lake Naleng on the north-eastern and south-eastern Tibetan Plateau, respectively, as well as Lake Zigetang on the central and Lake Bangong on the western Tibetan Plateau.

Lake Qinghai (36.55° N, 100.1° E, 3200 m a.s.l.) has a surface area of about 4400 km² and is the largest saline lake in China. Located at the north-eastern Tibetan Plateau and therewith in the fringe area of the Asian monsoon, the climate around the lake is influenced by three planetary-scale circulation systems: The region is not only characterised by the East Asian and Indian monsoon, but also affected by the westerly atmospheric flow (Xu et al., 2007). Thus, changes in climate, in particular the monsoon intensity, probably have a strong impact on the regional vegetation

Holocene vegetation and biomass changes on the Tibetan Plateau

A. Dallmeyer et al.

Title Page

Abstract

Introduction

Conclusions

References

Tables

Figures

⏪

⏩

◀

▶

Back

Close

Full Screen / Esc

Printer-friendly Version

Interactive Discussion



Holocene vegetation and biomass changes on the Tibetan Plateau

A. Dallmeyer et al.

Title Page

Abstract

Introduction

Conclusions

References

Tables

Figures

⏪

⏩

◀

▶

Back

Close

Full Screen / Esc

Printer-friendly Version

Interactive Discussion

composition. Nowadays, the lake lies in the semi-arid and moderate cold climate zone with mean annual precipitation and temperature reaching approx. 250 mm yr^{-1} and -0.7°C , respectively (Shen et al., 2005). The vegetation immediately around the lake is characterised by temperate steppes dominated by *Artemisia* and *Poaceae*. The reconstructions used in this study are based on a 795 cm long core (QH-2000) from the south-eastern part of the lake. For further description of the study site, material and dating see Shen et al. (2005).

Lake Naleng (31.1°N , 99.75°E , 4200 m a.s.l.) is a medium-sized freshwater lake on the south-eastern Tibetan Plateau (area: 1.8 km^2). The pronounced relief and steep elevations in its environment lead to strong climatic and vegetational gradients. The climate around the lake is influenced by the Asian monsoon, yielding 90% of the annual precipitation (ca. 630 mm yr^{-1} at a near climate station). The mean annual temperature is presumably 1.6°C (Kramer et al., 2010). Lake Naleng is situated at the upper tree line composed of *Picea*; the (sub-)alpine vegetation is composed of shrubs such as *Potentilla*, *Spiraea*, *Rhododendron* intermixed with *Kobresia* dominated meadows. Due to its location, climate change, especially variability in temperature, is expected to cause strong shifts in regional vegetation. The vegetation trend at this site is analysed, based on the upper part of a 17.8 m-long sediment core. Details of the study site, materials and methods are described in Kramer et al. (2010).

Lake Zigetang (32°N , 90.9°E , ca. 4500 m a.s.l.) is a large saline lake (surface area ca. 190 km^2) on the high-altitude inner Tibetan Plateau. The regional climate is cold and semi-arid, but still affected by the Indian monsoon circulation. Mean annual precipitation and temperature ranges from about $300\text{--}500 \text{ mm yr}^{-1}$ and from -2.6°C to -0.3°C , respectively. The vicinity of Lake Zigetang is covered by alpine steppe (dominated by *Poaceae* and *Artemisia*), but vegetation turns to alpine *Kobresia* meadows to the east of the lake. Further details are described in Herzschuh et al. (2006).

With a surface area of 604 km^2 , Lake Bangong (33.42°N , 79°E , 4200 m a.s.l.) is the largest lake on the western Tibetan Plateau. Located in the rain shadow of the

Kunlun and Karakorum mountain ranges, climate around the lake is cold and very dry. Annual mean temperature is ca. -1.5°C . Precipitation originates mainly from the Indian monsoon, but does not exceed 70 mm yr^{-1} (van Campo et al., 1996). Accordingly, montane desert/steppe-desert dominates the area characterised by a sparse vegetation cover. Pollen assemblages used in this study are based on a 12.4 m core from the eastern part of the lake. For further information on the material and site see van Campo et al. (1996) and Fontes et al. (1996).

3 Methods

3.1 Reconstruction

The qualitative interpretation of pollen assemblages in terms of past vegetation (Birks and Birks, 1980) can be validated using a quantitative method for pollen-based biome reconstruction (biomisation, Prentice et al., 1996). Based on knowledge of the contemporary biogeography and ecology of modern plants, pollen taxa are assigned to plant functional types (PFTs) and the PFTs are assigned to main vegetation types (biomes). An affinity score for each biome is then calculated according to Prentice et al. (1996). The biome with the highest score dominates in the pollen-source area of the lake, while a relatively lower score indicates less occurrence of a biome in the area. Scores cannot be compared between different records. The pollen taxa-biome matrix applied in this study is based on the standard biomisation procedure presented by Yu et al. (1998) and their later improved version (Yu et al., 2000). A test of this method with a modern pollen data set of 112 lake sediment-derived pollen spectra from the Tibetan Plateau yielded reasonable results (Herzschuh et al., 2010a). Here, we summarised the different biomes so that they fit best to the modelled vegetation types, namely forest, shrub, steppe/meadow and desert.

Holocene vegetation and biomass changes on the Tibetan Plateau

A. Dallmeyer et al.

Title Page

Abstract

Introduction

Conclusions

References

Tables

Figures



Back

Close

Full Screen / Esc

Printer-friendly Version

Interactive Discussion



3.2 General model setup and experimental design

To estimate the mid- to late-Holocene vegetation change on the Tibetan Plateau a transient numerical experiment was analysed. The simulation was performed by Fischer et al. (2011) with the comprehensive Earth system model ECHAM5/JSBACH-MPIOM, developed at the Max-Planck-Institute for Meteorology. The model consisted of the atmospheric general circulation model ECHAM5 (Roeckner et al., 2003) coupled to the land-surface-scheme JSBACH (Raddatz et al., 2007) and the ocean model MPIOM (Marsland et al., 2003; Jungclaus et al., 2006). JSBACH included the dynamic vegetation module of Brovkin et al. (2009). ECHAM5 ran with 19 vertical levels and a spectral resolution of T31, which corresponds to a latitudinal distance of ca. 3.75°, i.e. a grid-box width of about 354 km at 32° N. The ocean-grid had a horizontal resolution of approximately 3° and 40 vertical levels. The models have been tested against observation and reanalysis data proving that they capture the major structure of global and regional climate (e.g. Cui et al., 2006).

The transient experiment started at mid-Holocene climate conditions. Orbital parameters in the coupled models had been adjusted to the configuration 6000 years before present (further referred to as 6k). Atmospheric composition had been fixed at pre-industrial values with CO₂-concentration set to 280 ppm. Under these boundary conditions, the model was brought to quasi-equilibrium climate state. Afterwards, the orbital configuration was continuously being changed until present-day (0k) conditions were reached. During the entire transient run, atmospheric composition stayed constant. The calculated climate change, thus, can be attributed to orbital forcing alone. Biogeochemical processes have no influence.

Due to the coarse model resolution, it was not possible to take the geographically nearest grid-boxes around the lakes for the comparison of model results and reconstructions. Simulated present-day climate may differ strongly from observations, since the orography in the model is underestimated. Instead we chose grid-boxes in the vicinity of each lake, showing an analogue vegetation trend and more appropriate climate (Fig. 2).

Holocene vegetation and biomass changes on the Tibetan Plateau

A. Dallmeyer et al.

Title Page

Abstract

Introduction

Conclusions

References

Tables

Figures



Back

Close

Full Screen / Esc

Printer-friendly Version

Interactive Discussion



3.3 Dynamic vegetation module

The dynamic vegetation module used in this study distinguishes eight plant-functional types (PFTs), i.e. plants are grouped with regard to their physiology including their leaf phenology type. Trees can be either tropical or extratropical and are further differentiated between evergreen and deciduous trees. The module considers two shrubby vegetation types, namely raingreen shrubs and cold shrubs. The first is limited by moisture; the second represents shrubs limited by temperature. Grass is classified as either C3 or C4 grass.

For each PFT, environmental constraints are defined in the form of temperature thresholds representing their respective bioclimatic tolerance. These thresholds define the area, where establishment of a PFT is possible. They describe cold resistance by the lowest mean temperature of the coldest month ($T_{c_{min}}$), chilling requirements by the maximum mean temperature of the coldest month ($T_{c_{max}}$) and heat requirement for the growth phase. The latter is considered via the summation of temperature over days with temperature higher than 5°C , called growing degree days (GDD5). Cold shrubs are also excluded in regions with warm climate ($T_{w_{max}}$). The values of the limits are listed in Table 1 and similar to the limits used in the biosphere model LPJ (Sitch et al., 2003).

For each grid-box of the atmosphere, the land surface is tiled in mosaics, so that several PFTs can be represented in a single grid cell. The fractional cover of each PFT is determined by the balance of their establishment and mortality. The latter is the sum of the mortality by the aging of plants and the disturbance-related mortality (fire and windbreak). The establishment is calculated from the relative differences in annual net primary productivity (NPP) between the PFTs and hence includes the different moisture requirements of the plants. Furthermore, the establishment is weighted by the inverse of the PFT specific lifetime, i.e. plants that live long establish slowly. The establishment of woody PFTs is favoured over grass, so that grass can only establish in the area, which is left after trees and shrubs have established. In the absence of disturbances,

CPD

7, 1073–1111, 2011

Holocene vegetation and biomass changes on the Tibetan Plateau

A. Dallmeyer et al.

Title Page

Abstract

Introduction

Conclusions

References

Tables

Figures

⏪

⏩

◀

▶

Back

Close

Full Screen / Esc

Printer-friendly Version

Interactive Discussion

Holocene vegetation and biomass changes on the Tibetan Plateau

A. Dallmeyer et al.

Title Page

Abstract

Introduction

Conclusions

References

Tables

Figures

⏪

⏩

◀

▶

Back

Close

Full Screen / Esc

Printer-friendly Version

Interactive Discussion



woody PFTs thus have an advantage over grasses and the woody PFT with the highest NPP becomes the dominant vegetation-type in the grid-box. Generally, trees have the highest NPP, since they have the largest leaf-area. However, in regions with frequent disturbances or in unfavourable climate conditions, i.e. bioclimatic conditions near the thresholds, shrubs or even grass might win the competition as they can recover more quickly than trees.

For each grid cell, a non-vegetated area is considered as well, which represents the fraction of seasonally bare soil and permanently bare ground (deserts). Their fraction is calculated via the relation of maximum carbon storage in the pool representing living tissues to the carbon actually stored in this pool. This approach is based on the fact that plants need a certain amount of carbon to build their leaves, fine roots, etc., so that they can function properly. If the model calculates a positive NPP for a vegetation type, carbon is filled into this pool while carbon is lost from it proportional to the loss of leaves, which mostly happens in dry or cold seasons/periods. If the filling of the pool is not sufficient for all PFTs, plants cannot grow and the grid-cell is mainly non-vegetated.

Simulated changes in vegetation cover thus can be attributed to bioclimatic shifts, changes in plant productivity or changes in the frequency of disturbances. More details about the dynamic vegetation module are described in Brovkin et al. (2009).

In this study, PFTs are further aggregated to the three major vegetation types “forest” (containing all trees), “shrub” and “grass”. The fourth land cover type “desert” includes the non-vegetated area.

4 Results

The reconstructed biome trends (forest, shrubland, steppe/meadow, desert) for all sites are illustrated in Fig. 3. Figure 4 shows the corresponding simulated vegetation trend as averages over 20 years. Thereby, the simulated land cover is divided into forest, shrub and grass fraction as well as non-vegetated area, which is further referred to as desert. Simulated climate and vegetation changes are attributed to orbital forcing alone.

Holocene vegetation and biomass changes on the Tibetan Plateau

A. Dallmeyer et al.

[Title Page](#)

[Abstract](#)

[Introduction](#)

[Conclusions](#)

[References](#)

[Tables](#)

[Figures](#)

[⏪](#)

[⏩](#)

[◀](#)

[▶](#)

[Back](#)

[Close](#)

[Full Screen / Esc](#)

[Printer-friendly Version](#)

[Interactive Discussion](#)



The pollen record of Lake Qinghai (north-eastern Tibetan Plateau) reveals a continuous decrease of forest cover since the mid-Holocene (6k) and an expansion of steppe/meadow vegetation. Whereas forests and steppe/meadow dominated the land-cover at 6k, steppe/meadow is the prevalent biome at present-day (0k). Shrub vegetation, as well as desert vegetation, covers only small areas and does not show obvious trends through time. In line with the reconstructions of Qinghai Lake, the simulated vegetation trend on the north-eastern Tibetan Plateau (NETP) shows a continuous forest decline and an expansion of grassland during the last 6000 years. Forest as the dominating land cover type during the mid-Holocene (approx. 38% of the area) is halved until present-day. Grass and shrub fractions increase by 67% and 64%, covering 38% and 19% of the area at 0k, respectively. Thus, grass is the prevalent vegetation simulated and reconstructed for the north-eastern Tibetan Plateau at present-day. The desert fraction slightly decreases from 27% at 6k to 23% at 0k.

The pollen-based vegetation reconstruction from Lake Naleng (south-eastern Tibetan Plateau) suggests a qualitatively similar vegetation trend. During the mid-Holocene, steppe/meadow and forest were the dominant biomes. Around 4.3k, forests started to retreat and were replaced by steppes and meadows. Thus, pollen abundances clearly reveal that steppe and meadow vegetation dominate in the area of Lake Naleng for present-day. Desert and shrub vegetation have stayed low constantly since 6k. The simulated mid-Holocene land-cover on the south-eastern Tibetan Plateau (SETP) mainly consists of forest (91%) and to a lesser extent of grass and shrubs (8% and 1%, respectively). This vegetation distribution is constant for nearly 1200 years until shrubs successively replace forest. This decrease of forest fraction agrees with the reconstruction from Lake Naleng, but in the reconstructions steppe/meadow and not shrub fraction increase. A strong fluctuation in the modelled vegetation trend indicates an occasionally recovering tree fraction. At 0k, shrub is the dominant land cover type according to the model (60% of the area), while forests form only 32% of the landscape. Desert (0%) as well as grass fraction stay constant for the whole 6000 years.

Holocene vegetation and biomass changes on the Tibetan Plateau

A. Dallmeyer et al.

Title Page

Abstract

Introduction

Conclusions

References

Tables

Figures

⏪

⏩

◀

▶

Back

Close

Full Screen / Esc

Printer-friendly Version

Interactive Discussion

Lake Zigetang is situated on the high-altitude central Tibetan Plateau. At 6k as well as 0k, the area is primarily covered by steppe/meadow vegetation. The reconstructed Holocene vegetation change is small, but exhibits a slight tendency of increasing steppe/meadow vegetation. The occurrence of desert is highly variable. Shrub and tree pollen taxa occur with low but steady abundances. In contrast to the pollen record, the model simulates no forests and no shrubs on the central Tibetan Plateau (CTP) for the last 6000 years. Like in the reconstructions, grass covers most of the area at 6k (86%) as well as at 0k (85%). The simulated vegetation trend is small. However, grassland is slightly retreating during the first 3000 years (to 80% at 3k) and increasing again afterwards.

The pollen record of Lake Bangong from the western Tibetan Plateau depicts a regional vegetation decline during the last 6000 years. Forest, as well as steppe/meadow vegetation, has decreased, desert indicating plants have spread since the mid-Holocene. Whereas steppe was the dominant biome at 6k, pollen concentrations suggest land coverage of desert and steppe in equal parts for present-day. In agreement to the reconstructions from Lake Bangong, the model calculates an overall decrease of vegetated area on the central-western Tibet Plateau (CWTP). Whereas grass (41%) and forest (31%) characterise the landscape during the mid-Holocene, desert (43%) dominates the region at present-day. Simulated forest fraction is nearly halved, desert fraction more than doubled during the last 6000 years. Shrub and grass only decrease by ca. 15%, respectively.

5 Discussion

5.1 Potential reasons for disagreements in the simulated and reconstructed vegetation cover

The pollen-based vegetation reconstructions in this study may be influenced by the following factors:

not represent a true shift in the dominant biome but may simply reflect some ecological noise.

The simulated vegetation trend is limited by the following factors:

1. Due to the coarse numerical resolution (T31L19), the orography is not represented well in the model. This especially applies to the Tibetan Plateau. Whereas its mean elevation exceeds 4000 m in reality, orography in the model reaches 4000 m at most and only in a few grid-boxes on the central Tibetan Plateau. The Himalaya and the Kunlun Mountains, as well as other mountain ranges, vanish. In reality, the strong relief implies a high heterogeneity of regional climate and vegetation, which cannot be captured in the model and may lead to discrepancies between the model results and reconstructions.
2. Compared to annual mean 2-m-temperatures of European Centre for Medium-Range Weather Forecast Reanalysis (ERA40; Simmons and Gibson, 2000), simulated climate is too warm on the northern and too cold (up to -2.8°C) on the central and south-eastern Tibetan Plateau (see Fig. 5). Maximal positive temperature anomalies of up to 7.2°C occur on the western Tibetan Plateau. These differences between the model and reanalysis-data may partly arise from a lower (pre-industrial) greenhouse-gas concentration in the model. The comparison of the model output with observations (here: Global Precipitation Climatology Project (GPCP); Adler et al., 2003) also shows that the Asian summer monsoon intensity is overestimated in the central and southern regions of the Tibetan Plateau (see Fig. 5). Summer (JJA) precipitation anomalies reach values of up to ca. 7.5 mm day^{-1} . The simulated vegetation depends on certain climate thresholds, e.g. bioclimatic limiting factors. Therefore, biases in the calculated climate may lead to errors in the vegetation distribution and vegetation trend, particularly if the simulated local climate is near these thresholds, where sensitivity of land cover to climate change is expected to be large.

Holocene vegetation and biomass changes on the Tibetan Plateau

A. Dallmeyer et al.

Title Page

Abstract

Introduction

Conclusions

References

Tables

Figures

⏪

⏩

◀

▶

Back

Close

Full Screen / Esc

Printer-friendly Version

Interactive Discussion



Holocene vegetation and biomass changes on the Tibetan Plateau

A. Dallmeyer et al.

Title Page

Abstract

Introduction

Conclusions

References

Tables

Figures

⏪

⏩

◀

▶

Back

Close

Full Screen / Esc

Printer-friendly Version

Interactive Discussion

3. Anthropogenic land cover change is another potential source of error as this cannot be depicted with our model configuration, but may be included in the reconstructions. Nomadic people may have influenced the mid-Holocene land-cover on the Tibetan Plateau, at least on lower elevations. The earliest Neolithic settlement on the south-eastern Tibetan Plateau took place at an age between 6.5k and 5.6k (Aldenderfer, 2007). Humans lived on the margin of the north-eastern Tibetan Plateau at least seasonally during the period 9k–5k (Rhode et al., 2007). The expansion of Neolithic cultures coincides well with the forest decline in regions north-east of the Tibetan Plateau (Aldenfelder and Zhang, 2004; Brantingham and Gao, 2006) and in China (e.g. Ren, 2000). To what extent humans influenced the Holocene vegetation change on the Tibetan Plateau is still a matter of discussion (Schlütz and Lehmkuhl, 2009; Herzsuh et al., 2010b).

5.2 Site-specific discussion of the vegetation change

In the following, the indices “ann”, “wm” and “cm” stand for annual, warmest month and coldest month, respectively. The indices “0k” and “6k” denotes the simulated present-day and mid-Holocene climate, respectively.

5.2.1 North-eastern Tibetan Plateau

The simulated present-day climate on the north-eastern Tibetan Plateau is dry and cold. Annual mean precipitation ($p_{\text{ann}0\text{k}}$) and temperature ($T_{\text{ann}0\text{k}}$) are 230 mm yr^{-1} and -1.8°C , respectively. Thus, the calculated mean climate is in general agreement with observations around Lake Qinghai ($T_{\text{ann}} = -0.7^\circ\text{C}$, $p_{\text{ann}} = 250 \text{ mm yr}^{-1}$). Simulated temperatures range from $T_{\text{cm}0\text{k}} = -15.3^\circ\text{C}$ in the coldest month to $T_{\text{wm}0\text{k}} = 9.3^\circ\text{C}$ in the warmest month. Therefore, the only possible woody PFTs are cold shrubs and extratropical forests. At 6k as well as 0k, the bioclimatic conditions of these PFTs are only partly fulfilled, because the limit for the growing degree days above 5°C is not always reached (Fig. 6). Due to the warmer summer season during the

mid-Holocene ($T_{\text{wm6k}} = 10.6^{\circ}\text{C}$) compared to present-day, trees can grow easier at that time. The extension of the growth phase, as well as the higher amount of precipitation ($p_{\text{ann6k}} = 290 \text{ mm yr}^{-1}$), provides a more favourable climate for trees. The orbitally-induced gradual cooling towards the present-day results in a decline of forest and an increase of grass.

The similarity between the simulated and reconstructed vegetation trend suggests a natural climate change (summer insolation) as the main driving factor for the decreasing forest fraction on the north-eastern Tibetan Plateau. The simulation confirms recent results of a rather minor role of human activity in forming the land cover change in the area (Herzschuh et al., 2010b). However, the model results clearly point out warm season temperatures (GDD5) as the controlling factor, whereas reconstructions identified monsoon intensity related precipitation changes as the primary explanation for the vegetation trend (Herzschuh et al., 2010b). Stable oxygen-isotope measurements performed on *ostracod* valves suggest a wetter climate during the early-Holocene (9k–6k), a strongly decreasing precipitation trend until 3k and rather stable conditions afterwards (X. Liu et al., 2007).

5.2.2 South-eastern Tibetan Plateau

Lake Naleng is located at an elevation of 4200 m, whereas the mean orography prescribed to the model reaches only 2600 m in SETP. Therefore, the simulated annual temperature and precipitation are highly overestimated ($p_{\text{ann0k}} = 1850 \text{ mm yr}^{-1}$, $T_{\text{ann0k}} = 11.1^{\circ}\text{C}$). Bioclimatic conditions ($T_{\text{cm0k}} = 1.6^{\circ}\text{C}$, $T_{\text{wm0k}} = 17.3^{\circ}\text{C}$) support growing of raingreen shrubs and extratropical forests as the only possible woody PFTs.

In this area, the model simulates a higher NPP for raingreen shrubs than for extratropical trees, so that the preferred land cover type would be shrubs. Due to less winter insolation at 6k, the region experiences a colder winter climate than at present-day ($T_{\text{cm6k}} = 0.8^{\circ}\text{C}$). Frost events occur regularly (see Fig. 7). Therefore, raingreen shrubs are excluded as mid-Holocene land cover due to less favourable bioclimatic conditions. With increasing winter insolation, the cold season becomes

Holocene vegetation and biomass changes on the Tibetan Plateau

A. Dallmeyer et al.

Title Page

Abstract

Introduction

Conclusions

References

Tables

Figures

⏪

⏩

◀

▶

Back

Close

Full Screen / Esc

Printer-friendly Version

Interactive Discussion



warmer and frost events rare. Given a higher NPP in the model, raingreen shrubs are then able to successively replace the evergreen trees. However, the vegetation cover fluctuates, because frost events still occur with lower frequency.

Whereas the pollen reconstructions show an increase of steppe/meadow towards present-day, the model calculates shrubs as the forests-replacing land cover type. This difference in vegetation trend may partly result from the strong temperature bias of the model. Given the observed annual mean temperature ($T_{\text{ann}} = 1.6^{\circ}\text{C}$), growth of shrubs would probably have been impossible during the entire 6000 years. Present-day land cover would primarily be forest.

Furthermore, human activity cannot be excluded from having an influence on the vegetation trend and modern distribution. Grazing indicators suggest human impact on the environment around Lake Naleng since 3.4k (Kramer et al., 2010). Thus, forest clearance as well as fire activity and grazing may have contributed to the forest decline on the south-eastern Tibetan Plateau (Schlütz and Lehmkuhl, 2009).

Pollen reconstructions assume decreasing summer temperatures as the major controlling climate factor, causing a downward shift of the treeline (Kramer et al., 2010). As Lake Naleng is situated in an area where forests gradually pass into subalpine shrub and alpine meadow, a transition from forest to shrubland during the Holocene would have been possible as well. Since shrub genera in that area, such as *Potentilla*, *Caragana*, *Spiraea*, *Rhododendron*, are poor pollen producers, shrubby vegetation may be underestimated in the vegetation reconstruction from Lake Naleng pollen spectra.

However, winter temperature is the main driving climate factor for the vegetation trend in the model. With regard to the discrepancy in local climate, the simulated vegetation trend should be interpreted in a broader sense: During the mid-Holocene, colder winters provided more unfavourable climatic conditions for frost-sensitive plants than at present-day. With increasing winter temperatures they might have had a chance to establish in spite of the pressure of other competitive, frost-resistant plants.

Holocene vegetation and biomass changes on the Tibetan Plateau

A. Dallmeyer et al.

Title Page

Abstract

Introduction

Conclusions

References

Tables

Figures



Back

Close

Full Screen / Esc

Printer-friendly Version

Interactive Discussion



5.2.3 Central Tibetan Plateau

The simulated climate on the central Tibetan Plateau is cold and relatively wet. Annual mean precipitation is overestimated by the model. It reaches 743 mm yr^{-1} , mainly provided by the Indian summer monsoon. With annual mean temperatures well below freezing point ($T_{\text{ann0k}} = -4.8^\circ\text{C}$), climate conditions are too cold to allow the establishment of woody PFTs. Even in the warm season, mean temperatures do not exceed 4.5°C . Therefore, the annual temperature sum is not high enough to fulfil the limit of growing degree days in the model.

These climate conditions have not changed much during the 6000 years of simulation. The calculated vegetation trend seems to follow the mean summer (JJA) temperature (Fig. 8). Lower temperatures around 3k yield a slight decrease of the grass fraction, indicating warm season temperatures as the controlling climate factor for the vegetation trend.

While the model simulates no forest and shrub on the central Tibetan Plateau, reconstructions for Lake Zigetang reveal a low pollen assemblage of these vegetation types. These pollens have apparently been transported from downstream-located regions.

Pollen reconstructions suggest a vegetation transition from *Artemisia*-dominated alpine steppe at 6k to *Kobresia*-dominated meadow at 0k (Herzschuh et al., 2006, 2010b) that was interpreted in terms of temperature decrease.

5.2.4 Central-western Tibetan Plateau

The simulated vegetation trend agrees well with the reconstructions from Lake Bangong, although the calculated climate highly differs from climate observations in the surrounding of this lake. Due to the flat orography in the model (mean height $<2000 \text{ m}$), simulated mean annual temperatures for present-day are 16.5°C instead of the observed -1.5°C . Moreover, the Indian monsoon intensity is slightly overestimated in that region. Annual mean precipitation reaches 250 mm yr^{-1} (observed: ca.

CPD

7, 1073–1111, 2011

Holocene vegetation and biomass changes on the Tibetan Plateau

A. Dallmeyer et al.

Title Page

Abstract

Introduction

Conclusions

References

Tables

Figures

⏪

⏩

◀

▶

Back

Close

Full Screen / Esc

Printer-friendly Version

Interactive Discussion



70 mm yr⁻¹). Bioclimatic conditions ($T_{cm0k} = 0.32\text{ }^{\circ}\text{C}$, $T_{wm0k} = 26.6\text{ }^{\circ}\text{C}$) support growth of extratropical forests and partly of raingreen shrubs. The latter are hindered by the occasional occurrence of frosts. However, due to its location at the southern margin of the Plateau and due to the low regional pollen productivity, the pollen source area of the lake may comprise large areas of lower elevations and is thus rather similar to the modelled vegetation for that region.

Reconstructions as well as the model results identify precipitation – being mainly a function of the Indian monsoon strength – as the main driver for the vegetation change. Calculated annual mean precipitation is halved between 6k ($p_{ann6k} = 500\text{ mm yr}^{-1}$) and 0k (see Fig. 9), resulting in an increase of desert fraction. Proxy data suggests a maximum of moisture availability between 7.2–6.5k and then a trend towards aridity (van Campo et al., 1996). Thus, climate reconstructions and model data both show a decrease of summer monsoon intensity on the western Tibetan Plateau during the last 6000 years.

5.3 Simulated total vegetation and biomass changes on the Tibetan Plateau

Table 2 illustrates the averaged simulated vegetation and biomass change on the Tibetan Plateau, which we defined as those grid-boxes exceeding orographic height of 2500 m in the model (cf. Fig. 2). This area has a size of approx. 3.43 million km².

Overall, the forest fraction decreases by nearly one third, i.e. an area of ca. 0.45 million km². Whereas forest covers approx. 41.4% of the Tibetan Plateau at mid-Holocene, only 28.3% area are covered by forests at present-day. Most of the forest has been replaced by shrubs, whose fraction is nearly four times larger at 0k (12.3% of the total area) than at 6k (ca. 3.2% of the total area). The area covered by grass increases from approx. 38.1% at mid-Holocene to 42.3% at present-day. Altogether, a small fraction of the Tibetan Plateau is more vegetated at present-day. Non-vegetated area is reduced from 17.29% at 6k to 17.16% at 0k.

Holocene vegetation and biomass changes on the Tibetan Plateau

A. Dallmeyer et al.

[Title Page](#)[Abstract](#)[Introduction](#)[Conclusions](#)[References](#)[Tables](#)[Figures](#)[⏪](#)[⏩](#)[◀](#)[▶](#)[Back](#)[Close](#)[Full Screen / Esc](#)[Printer-friendly Version](#)[Interactive Discussion](#)

Holocene vegetation and biomass changes on the Tibetan Plateau

A. Dallmeyer et al.

Title Page

Abstract

Introduction

Conclusions

References

Tables

Figures

⏪

⏩

◀

▶

Back

Close

Full Screen / Esc

Printer-friendly Version

Interactive Discussion

This vegetation change results in a relocation of carbon stored in the soil and plants. At mid-Holocene, approx. 2.8 kgC m^{-2} are stored in the vegetation, particularly in forests (2.7 kgC m^{-2}). Due to the forest decline from 6k to 0k, more than 1 kgC m^{-2} living biomass is released. Only half of this biomass loss is compensated by shrubs and, to a small extent, by grass. Therefore, the total living biomass loss on the Tibetan Plateau during the last 6000 years adds up to ca. 0.62 kgC m^{-2} , on average. The Holocene climate change from 6k to 0k and the associated degradation of vegetation thus lead to a plant carbon loss of nearly one quarter.

The vegetation change on the Tibetan Plateau also strongly affects the total terrestrial biomass, i.e. the biomass stored not only in plants but also in soil and litter. In mid-Holocene, approx. 18.7 kgC m^{-2} are fixed as terrestrial biomass. The reduction of area covered by forest yield a decrease of terrestrial carbon by more than 5 kgC m^{-2} . Forest-replacing shrubs and grassland can partly compensate this biomass loss. Nevertheless, the total terrestrial carbon loss on the Tibetan Plateau between the mid-Holocene and present-day exceeds 1.9 kgC m^{-2} on average. Projected on the total area of ca. 3.43 million km^2 (in the model), the terrestrial carbon loss adds up to 6.64 GtC.

6 Summary and conclusion

Pollen-inferred vegetation trends on the Tibetan Plateau since the mid-Holocene were compared to simulated land cover changes, conducted in a coupled atmosphere-ocean-vegetation model with orbital forcing only. As the Tibetan Plateau exhibits diverse environmental and climate conditions, four different pollen records were considered, representing different parts of the Tibetan Plateau. Causes of the vegetation change and consequences for the biomass storage have been investigated.

In general, simulated and reconstructed vegetation trends are in agreement for each site but way and manner differ regionally. The results of both methods indicate a degradation of the vegetation, particularly characterised by a strong decrease of

Holocene vegetation and biomass changes on the Tibetan Plateau

A. Dallmeyer et al.

Title Page

Abstract

Introduction

Conclusions

References

Tables

Figures

⏪

⏩

◀

▶

Back

Close

Full Screen / Esc

Printer-friendly Version

Interactive Discussion



forests. Simulated forest fraction is reduced by nearly one-third at present-day. Simulated total biomass on the Tibetan Plateau has decreased by ca. 6.64 GtC since the mid-Holocene. In some cases, however, model and reconstructions attribute this vegetation change to different climatic factors, which partly results from the fact that both methods have deficits. On the one hand, reconstructions might be affected by long-distance transports of pollen and the dependence of the pollen-production on the vegetation type and environmental conditions, including climate. Human influence probably cannot be neglected either. On the other hand, the coarse resolution of the model and the associated underestimation of the orography leads to discrepancies between the simulated present-day climate and observation.

On the north-eastern Plateau (Lake Qinghai, NETP), the model reveals orbitally-induced cooling of the warm season as the responsible climatic factor for the forest decline. Reconstructions, however, suggest the reduction of summer monsoon precipitation as the limiting factor. The model results might indicate that, so far, the influence of temperature changes on the Tibetan Plateau vegetation has been underestimated as an explanation for the decreasing forest in paleo-reconstructions for monsoon-affected areas.

The vegetation degradation around Lake Naleng (SETP) is caused by changes in temperature between mid-Holocene and present-day. According to reconstructions, decreasing summer temperatures lead to a downward shift of the treeline and therefore to less forest vegetation around Lake Naleng. The reduction of forest fraction in the model can be attributed to increasing winter temperature. Since the simulated climate for SETP strongly deviate from observation, this result should be interpreted with caution.

Harsh climatic conditions on the central Tibetan Plateau (Lake Zigetang) during the mid-Holocene as well as present-day lead to only slight vegetation changes in the model and in reconstructions.

The land cover degradation on the central-western Tibetan Plateau (Lake Bangong) can be attributed to a change in precipitation. Since the local climate is dry, the

reduction of summer monsoon precipitation from 6k to 0k causes an expansion of deserts and a dieback of vegetation in the model as well as in reconstructions.

Although the numerical resolution of the model is coarse and the experimental set-up is designed to analyse climate and vegetation changes due to orbital forcing alone, the model results agree with the reconstructed vegetation trend on the Tibetan Plateau.

Therefore, reconstructed large-scale land cover change since the mid-Holocene can likely be attributed to natural and not anthropogenic reasons, although humans might still have influenced the vegetation on a local scale strongly. The comprehensive Earth system model used in this study captures the regional climatic reasons for the vegetation change in most instances. Thus, it provides a good tool to understand the long-term vegetation change on the Tibetan Plateau as well as its causes and consequences.

However, the discrepancy between the simulated climate and observations in some parts of the Plateau show that the analysis-options are limited in simulations with coarse spatial resolution. Detailed analyses of important processes such as local changes of the energy balance or atmospheric flow are only possible in experiments with higher numerical resolution, where the complex terrain of the Tibetan Plateau is represented better.

Acknowledgements. The authors would like to thank E. van Campo, Xingqi Liu and A. Kramer for their pollen data contribution. Furthermore, we would like to thank T. Kleinen, MPI-M, and T. Raddatz, MPI-M, for constructive discussion. This research is part of the priority program INTERDYNAMIK funded by the German Research Foundation (DFG). This study also contributes to the Cluster of Excellence CliSAP (Integrated Climate System Analysis and Prediction) funded by the German Federal Government and the German States.

The service charges for this open access publication have been covered by the Max Planck Society.

Holocene vegetation and biomass changes on the Tibetan Plateau

A. Dallmeyer et al.

Title Page

Abstract

Introduction

Conclusions

References

Tables

Figures



Back

Close

Full Screen / Esc

Printer-friendly Version

Interactive Discussion



References

- Adler, R.F., Huffman, G. J., Chang, A., Ferraro, R., Xie, P., Janowiak, J., Rudolf, B., Schneider, U., Curtis, S., Bolvin, D., Gruber, A., Susskind, J., Arkin, P., Nelkin, E.: The Version 2 Global Precipitation Climatology Project (GPCP) Monthly Precipitation Analysis (1979–Present), *J. Hydrometeor.*, 4, 1147–1167, 2003.
- Aldenderfer, M. S.: Modeling the Neolithic on the Tibetan Plateau, in: Late Quaternary climate change and human adaptation in arid China, edited by: Madsen, D. B., Chen, F., and Gao, X., *Developements in Quaternary Science*, 151–166, 2007.
- Aldenderfer, M. and Zhang, Y.: The prehistory of the Tibetan Plateau to the seventh century A.D.: perspectives and research from China and the West since 1950, *J. World Prehist.*, 18, 1–55, 2004.
- Asnani, G. C.: Tropical meteorology, Published by G.C. Asnani, c/o Indian Institute of Tropical Meteorology, Noble Printers, Pashan, Pune-411008, India, 1–2, 1202 pp., 1993.
- Birks, H. J. B. and Birks, H. H.: Quaternary palaeoecology, Edward Arnold, 1980.
- Brantingham, P. J. and Gao, X.: Peopling of the northern Tibetan Plateau, *World Archaeol.*, 38, 387–414, 2006.
- Brovkin, V., Raddatz, T., Reick, C. H., Claussen, M., and Gayler, V.: Global biogeophysical interactions between forest and climate, *Geophys. Res. Lett.*, 36, L07405, doi:10.1029/2009GL037543, 2009.
- Claussen, M., Brovkin, V., and Ganopolski, A.: Biogeophysical versus biogeochemical feedbacks of large-scale land cover change, *Geophys. Res. Lett.*, 28(6), 1011–1014, 2001.
- Cui, X. and Graf, H. F.: Recent land cover changes on the Tibetan Plateau: a review, *Climatic Change*, 94, 47–61, 2009.
- Cui, X., Graf, H. F., Langmann, B., Chen, W., and Huang, R.: Climate impacts of anthropogenic land use changes on the Tibetan Plateau, *Glob. Planet. Change*, 54, 33–56, 2006.
- Duan, A. and Wu, G. X.: Role of the Tibetan Plateau thermal forcing in the summer climate pattern over subtropical Asia, *Clim. Dyn.*, 24, 793–807, 2005.
- Fischer, N. and Jungclaus, J. H.: Evolution of the seasonal temperature cycle in a transient Holocene simulation: orbital forcing and sea-ice, *Clim. Past Discuss.*, 7, 463–483, doi:10.5194/cpd-7-463-2011, 2011.
- Fontes, J., Gasse, F., and Gibert, E.: Holocene environmental changes in Lake Bangong basin (Western Tibet), Part 1: Chronology and stable isotopes of carbonates of a Holocene

Holocene vegetation and biomass changes on the Tibetan Plateau

A. Dallmeyer et al.

Title Page

Abstract

Introduction

Conclusions

References

Tables

Figures

⏪

⏩

◀

▶

Back

Close

Full Screen / Esc

Printer-friendly Version

Interactive Discussion



Holocene vegetation and biomass changes on the Tibetan Plateau

A. Dallmeyer et al.

Title Page

Abstract

Introduction

Conclusions

References

Tables

Figures

⏪

⏩

◀

▶

Back

Close

Full Screen / Esc

Printer-friendly Version

Interactive Discussion



- lacustrine core, *Palaeogeogr. Palaeoclimatol.*, 120(1–2), 25–47, 1996.
- Gasse, F., Arnold, M., Fontes, J. Ch., Fort, M., Gibert, E., Huc, A., Bingyan, L., Yuanfang, L., Qing, L., Mélières, F., Van Campo, E., Fubao, W., and Qingsong, Z.: A 13 000 yr climate record from Western Tibet, *Nature*, 353, 742–745, doi:10.1038/353742a0, 1991.
- 5 Gehrig, R. and Peeters, A. G.: Pollen distribution at elevations above 1000 m in Switzerland, *Aerobiologia*, 16, 69–74, 2000.
- Herzschuh, U., Winter, K., Wünnemann, B., and Li, S.: A general cooling trend on the central Tibetan Plateau throughout the Holocene recorded by the Lake Zige tang pollen spectra, *Quat. Int.*, 154–155, 113–121, 2006.
- 10 Herzschuh, U., Birks, H. J. B., Mischke, S., Zhang, C., and Böhner, J.: A modern pollen-climate calibration set based on lake sediments from the Tibetan Plateau and its application to a Late Quaternary pollen record from the Qilian Mountains, *J. Biogeogr.*, 37, 752–766, 2010a.
- Herzschuh, U., Birks, H. J. B., Ni, J., Zhao, Y., Liu, H., Liu, X., and Grosse, G.: Holocene land-cover changes on the Tibetan Plateau, *Holocene*, 20, 91–104, 2010b.
- 15 Hou, X. (Chief Ed.): *Vegetation atlas of China*, Science Press, Beijing, 2001.
- Hsu, H.-H. and Liu, X.: Relationship between the Tibetan Plateau heating and East Asian summer monsoon rainfall, *Geophys. Res. Lett.*, 30(20), 2066, doi:10.1029/2003GL017909, 2003.
- Jacobson Jr., G.L. and Bradshaw, R. H. W.: The selection of sites for paleovegetational studies, *Quat. Res.*, 16, 80–96, 1981.
- 20 Jungclaus, J. H., Botzet, M., Haak, H., Keenlyside, N., Luo, J.-J., Latif, M., Marotzke, J., Mikolajewicz, U., and Roeckner, E.: Ocean circulation and tropical variability in the coupled model ECHAM5/MPI-OM, *J. Climate*, 19, 3952–3972, 2006.
- Kramer, A., Herzschuh, U., Mischke, S., and Zhang, C.: Holocene treeline shifts and monsoon variability in the Hengduan Mountains (southeastern Tibetan Plateau), implications from palynological investigations, *Palaeogeogr., Palaeoclimatol.*, 286(1–2), 23–41, 2010.
- 25 Liu, X., Shen, J., Wang, S., Wang, Y., and Liu, W.: Southwest monsoon changes indicated by oxygen isotope of ostracode shells from sediments in Qinghai Lake since the late Glacial, *Chinese Sci. Bull.*, 52, 539–544, 2007.
- 30 Liu, Y. M., Bao, Q., Duan, A. M., Qian, Z. A., and Wu, G. X.: Recent progress in the impact of the Tibetan Plateau on climate in China, *Adv. Atmos. Sci.*, 24, 1060–1076, 2007.
- Markgraf, V.: Pollen dispersal in a mountain area, *Grana*, 19, 127–146, 1980.
- Marsland, S. J., Haak, H., Jungclaus, J. H., Latif, M., and Roske, F.: The Max-Planck-Institute

Holocene vegetation and biomass changes on the Tibetan Plateau

A. Dallmeyer et al.

Title Page

Abstract

Introduction

Conclusions

References

Tables

Figures

⏪

⏩

◀

▶

Back

Close

Full Screen / Esc

Printer-friendly Version

Interactive Discussion



global ocean/sea ice model with orthogonal curvilinear coordinates, *Ocean Modell.*, 5, 91–127, 2003.

Prentice, I. C., Guiot, J., Huntley, B., Jolly, D., and Cheddadi, R.: Reconstructing biomes from palaeological data: a general method and its application to European pollen data at 0 and 6ka, *Clim. Dynam.*, 12, 185–94, 1996.

Raddatz, T. J., Reick, C. H., Knorr, W., Kattge, J., Roeckner, E., Schnur, R., Schnitzler, K.-G., Wetzol, P., and Jungclaus, J.: Will the tropical land biosphere dominate the climate-carbon cycle feedback during the twenty-first century?, *Clim. Dynam.*, 29, 565–574, 2007.

Ren, G.: Decline of the mid- to late Holocene forests in China: climatic change or human impact?, *J. Quaternary Sci.*, 15(3), 273–281, 2000.

Rhode, D., Zhang, H. Y., Madsen, D. B., Xing, G., and Brantingham, R. J., Ma, H. Z., and Olsen, J. W.: Epipaleolithic/early Neolithic settlements at Qinghai Lake, western China, *J. Archaeol. Sci.*, 34, 600–612, 2007.

Rodwell, M. and Hoskins B.: Monsoons and the dynamics of deserts, *Quart. J. Roy. Meteor. Soc.*, 122, 1385–1404, 1996.

Roeckner, E., Bäuml, G., Bonaventura, L., Brokopf, R., Esch, M., Giorgetta, M., Hagemann, S., Kirchner, I., Kornblueh, L., Manzini, E., Rhodin, A., Schlese, U., Schultzweida, U., and Tompkins, A.: The atmospheric general circulation model ECHAM5, Part I: Model description, *MaxPlanckInst. f. Meteor., Report No. 349, Hamburg*, 2003.

Schlütz, F. and Lehmkuhl, F.: Holocene climatic change and the nomadic Anthropocene in Eastern Tibet: palynological and geomorphological results from the Niabooyeze Mountains, *Quat. Sci. Rev.*, 28(15–16), 1449–1471, doi:10.1016/j.quascirev.2009.01.009, 2009.

Shen, J., Liu, X., Wang, S., and Ryo, M.: Paleoclimatic changes in the Qinghai Lake area during the last 18 000 years, *Quat. Int.*, 136, 131–140, 2005.

Shen, J., Jones, R. T., and Yang, X.: The Holocene vegetation history of Lake Erhai, Yunnan Province southwestern China: the role of climate and human forcings, *Holocene*, 16, 265–276, 2006.

Simmons, A. J. and Gibson, J. K.: The ERA-40 Project Plan, ERA-40 Project Report Series No. 1 ECMWF, Shinfield Park, Reading, UK, 63 pp., 2000.

Sun, H. (Chief Ed.): The national physical atlas of China, China Cartographic Publishing House, 230 pp., 1999.

Sitch, S., Smith, B., Prentice, I. C., Arneeth, A., Bondeau, A., Cramer, W., Kaplan, J. O., Levis, S., Lucht, W., Sykes, M. T., Thonicke, K., Venevsky, S.: Evaluation of ecosystem dynamics,

Holocene vegetation and biomass changes on the Tibetan Plateau

A. Dallmeyer et al.

Title Page

Abstract

Introduction

Conclusions

References

Tables

Figures

⏪

⏩

◀

▶

Back

Close

Full Screen / Esc

Printer-friendly Version

Interactive Discussion

plant geography and terrestrial carbon cycling in the LPJ dynamic global vegetation model, *Glob. Change Biol.*, 9, 161–185, 2003.

Tang, L. Y., Shen, C. M., Li, C. H., Peng, J. L., Liu, H., Liu, K. B., Morrill, C., Overpeck, J. T., Cole, J. E., Yang, B.: Pollen-inferred vegetation and environmental changes in the central Tibetan Plateau since 8200 yr BP, *Sci. China Ser. D-Earth Sci.*, 52(8), 1104–1114, doi:10.1007/s11430-009-0080-5, 2009.

Ueno, K., Fujii, H., Yamada, H., and Liu, L.: Weak and frequent monsoon precipitation over the Tibetan Plateau, *J. Meteorol. Soc. Jpn.*, 79(1B), 419–434, 2001.

Van Campo, E., Cour, P., and Sixuan, H.: Holocene environmental changes in Bangong Co basin (Western Tibet), Part 2: The pollen record, *Palaeogeogr. Palaeoclimatol.*, 120(1–2), 49–63, 1996.

Wang, B., Bao, Q., Hoskins, B., Wu, G. X., and Liu, Y.: Tibetan Plateau warming and precipitation changes in East Asia, *Geophys. Res. Lett.*, 35(14), L14702, doi:10.1029/2008GL034330, 2008.

Wu, G. X.: Recent advances in Qinghai-Xizhang-Plateau climate dynamic research, *Quart. Sci.*, 24(1), 1–9, 2004 (in Chinese).

Wu, G. X. and Zhang, Y. S.: Tibetan Plateau forcing and the timing of the monsoon onset over South Asia and the South China Sea, *Mon. Weather Rev.*, 126, 913–927, 1998.

Wu, G. X., Wang, J., Liu, X., and Liu, Y. M.: Numerical modelling of the influence of Eurasian orography on the atmospheric circulation in different seasons, *Acta Meteorol. Sin.*, 63(5), 603–612, 2005 (in Chinese).

Wu, G. X., Liu, Y. M., Wang, T. M., Wan, R., Liu, X., Li, W., Wang, Z., Zhang, Q., Duan, A., and Liang, X.: The influence of the mechanical and thermal forcing of the Tibetan plateau on the Asian climate, *J. Hydrometeorol.*, 8, 770–789, 2007.

Xu, H., Hou, Z. H., Ai, L., and Tan, L. C.: Precipitation at Lake Qinghai, NE Qinghai-Tibet Plateau, and its relation to Asian summer monsoons on decadal/ interdecadal scales during the past 500 years, *Palaeogeogr. Palaeoclimatol.*, 254, 541–549, 2007.

Yanai, M. and Wu, G. X.: Effects of the Tibetan Plateau, *The Asian Monsoon*, edited by: Wang, B., Springer, 513–549, 2006.

Yasunari, T.: Role of Land-Atmosphere Interaction on Asian Monsoon Climate, *J. Meteorol. Soc. Jpn.*, 85B, 55–75, 2007.

Ye, D. Z. and Wu, G. X.: The role of the heat source of the Tibetan Plateau in the general circulation, *Meteorol. Atmos. Phys.*, 67, 181–198, 1998.

Holocene vegetation and biomass changes on the Tibetan Plateau

A. Dallmeyer et al.

Title Page

Abstract

Introduction

Conclusions

References

Tables

Figures

⏪

⏩

◀

▶

Back

Close

Full Screen / Esc

Printer-friendly Version

Interactive Discussion



Yu, G., Prentice, I. C., Harrison, S. P., and Sun, X.: Pollen-based biome reconstruction for China at 0 and 6000 years, *J. Biogeogr.*, 25, 1055–1069, 1998.

Yu, G., Chen, X., Ni, J., Cheddadi, R., Guiot, J., Han, H., Harrison, S. P., Huang, C., Ke, M., Kong, Z., Li, S., Li, W., Liew, P., Liu, G., Liu, J., Liu, Q., Liu, K.-B., Prentice, I.C., Qui, W., Ren, G., Song, C., Sugita, S., Sun, X., Tang, L., Van Campo, E., Xia, Y., Xu, Q., Yan, S., Yang, X., Zhao, J.; and Zheng, Z.: Palaeovegetation of China: a pollen date-based synthesis for the mid-Holocene and last glacial maximum, *J. Biogeogr.*, 27, 635–664, 2000.

Zhang, Q. Y., Jin, Z. H., and Peng, J. B.: The relationship between convection over the Tibetan Plateau and circulation over East Asia, *Chinese J. Atmos. Sci.*, 30, 802–812, 2006 (in Chinese).

Holocene vegetation and biomass changes on the Tibetan Plateau

A. Dallmeyer et al.

Table 1. Bioclimatic limits for the 8 plant functional types (PFTs) used in the coupled model experiment. Listed are phenology type, PFT-specific minimum of coldest monthly mean temperature ($T_{c_{\min}}$), PFT-specific maximum of coldest monthly mean temperature ($T_{c_{\max}}$), PFT-specific maximum warmest monthly mean temperature ($T_{w_{\max}}$) and growing degree days, i.e. temperature sum of days with temperatures exceeding 5 °C (GDD5). All temperature values are given in °C.

No.	Landcover classification	Phenology type	$T_{c_{\min}}$ (°C)	$T_{c_{\max}}$ (°C)	$T_{w_{\max}}$ (°C)	GDD5 (°C)
1	tropical evergreen trees	raingreen	15.5	–	–	0
2	tropical deciduous trees	raingreen	15.5	–	–	0
3	extratrop. evergreen trees	evergreen	–32.5	18.5	–	350
4	extratrop. deciduous trees	summergreen	–	18.5	–	350
5	raingreen shrubs	raingreen	0	–	–	900
6	cold shrubs	summergreen	–	–2	18	300
7	C3 grass	grasses	–	15	–	0
8	C4 grass	grasses	10	–	–	0

[Title Page](#)
[Abstract](#)
[Introduction](#)
[Conclusions](#)
[References](#)
[Tables](#)
[Figures](#)
[⏪](#)
[⏩](#)
[◀](#)
[▶](#)
[Back](#)
[Close](#)
[Full Screen / Esc](#)
[Printer-friendly Version](#)
[Interactive Discussion](#)


Holocene vegetation and biomass changes on the Tibetan Plateau

A. Dallmeyer et al.

Table 2. Total vegetation and biomass change on the Tibetan Plateau between mid-Holocene (6k) and present-day (0k), averaged over all grid-cells with orography exceeding 2500 m in the model (see Fig. 2). Listed are the area covered by the vegetation types and by vegetation in total (fraction of grid-cell in %), as well as living biomass, litter biomass, biomass allocated in the soil under the vegetation and total biomass. Biomass is given in gC m^{-2} .

	Vegetation			Forests			Shrubs			Grass		
	6k	0k	6k–0k	6k	0k	6k–0k	6k	0k	6k–0k	6k	0k	6k–0k
area (%)	82.71	82.84	–0.13	41.41	28.33	13.07	3.17	12.25	–9.09	38.14	42.25	–4.11
liv. biom. (gC m^{-2})	2778.45	2161.77	616.68	2700.28	1627.77	1072.51	48.95	502.64	–453.68	29.29	31.42	–2.12
litt. biom. (gC m^{-2})	1282.59	990.05	292.54	1139.06	699.24	439.82	26.26	160.00	–133.74	117.28	130.84	–13.56
soil biom. (gC m^{-2})	14661.54	13634.54	1027.00	9119.29	5576.78	3542.51	597.38	2297.47	–1700.08	4944.52	5760.40	–815.88
tot. biom. (gC m^{-2})	18722.00	16786.00	1936.00	12958.63	7903.79	5054.84	672.60	2960.11	–2287.51	5091.09	5922.66	–831.56

Title Page

Abstract

Introduction

Conclusions

References

Tables

Figures

⏪

⏩

◀

▶

Back

Close

Full Screen / Esc

Printer-friendly Version

Interactive Discussion

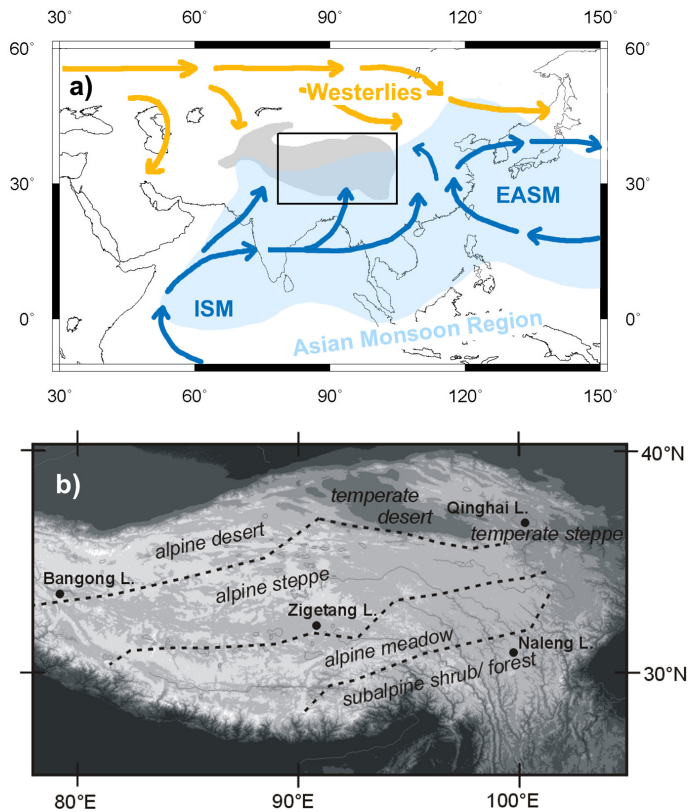


Fig. 1. (a) Sketch of the main atmospheric circulation systems affecting the Tibetan Plateau (grey-shaded) during the summer monsoon season: Westerly wind circulation (orange), Indian summer monsoon circulation (ISM, blue) and East Asian summer monsoon circulation (EASM, blue). Light blue shaded region marks the Asian monsoon domain; (b) shows the area marked as black rectangle in (a) and displays the distribution of the main vegetation types on the Tibetan Plateau (modified from Hou, 2001) and locations of the different study sites.

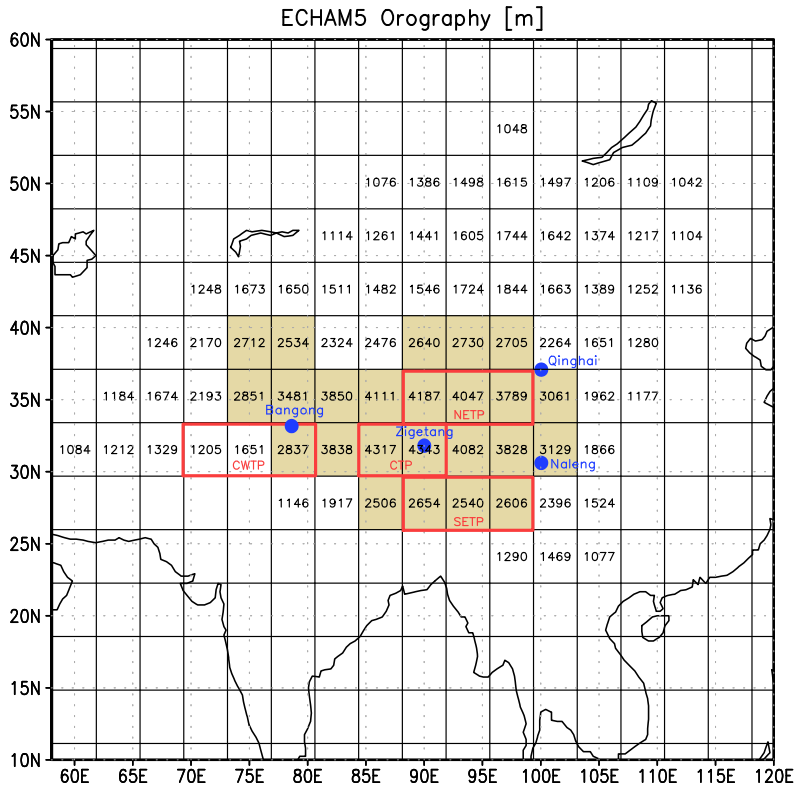


Fig. 2. ECHAM5 orography (elevation higher than 1000 m), model grid (T31) and grid boxes used for determining the averaged vegetation trend in four different regions on the Tibetan Plateau (red boxes). These are the north-eastern Tibetan Plateau (NETP), the south-eastern Tibetan Plateau (SETP), the central Tibetan Plateau (CTP) and the central-western Tibetan Plateau (CWTP). The locations of lakes sampled for vegetation reconstructions are also shown (blue dots). Shaded area marks the regions on the Tibetan Plateau which are elevated above 2500 m in the model.

Holocene vegetation and biomass changes on the Tibetan Plateau

A. Dallmeyer et al.

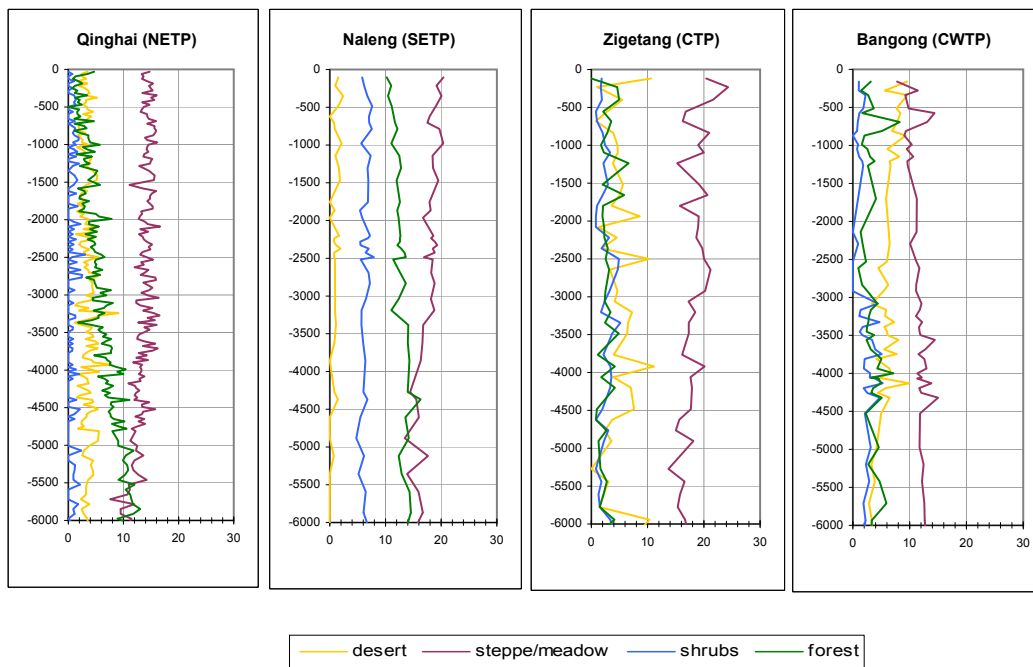


Fig. 3. Reconstructed vegetation trend from mid-Holocene (6000 years before present) to present-day, based on four different lake sediment cores on the Tibetan Plateau (in arbitrary units).

[Title Page](#)[Abstract](#)[Introduction](#)[Conclusions](#)[References](#)[Tables](#)[Figures](#)[⏪](#)[⏩](#)[◀](#)[▶](#)[Back](#)[Close](#)[Full Screen / Esc](#)[Printer-friendly Version](#)[Interactive Discussion](#)

Holocene vegetation and biomass changes on the Tibetan Plateau

A. Dallmeyer et al.

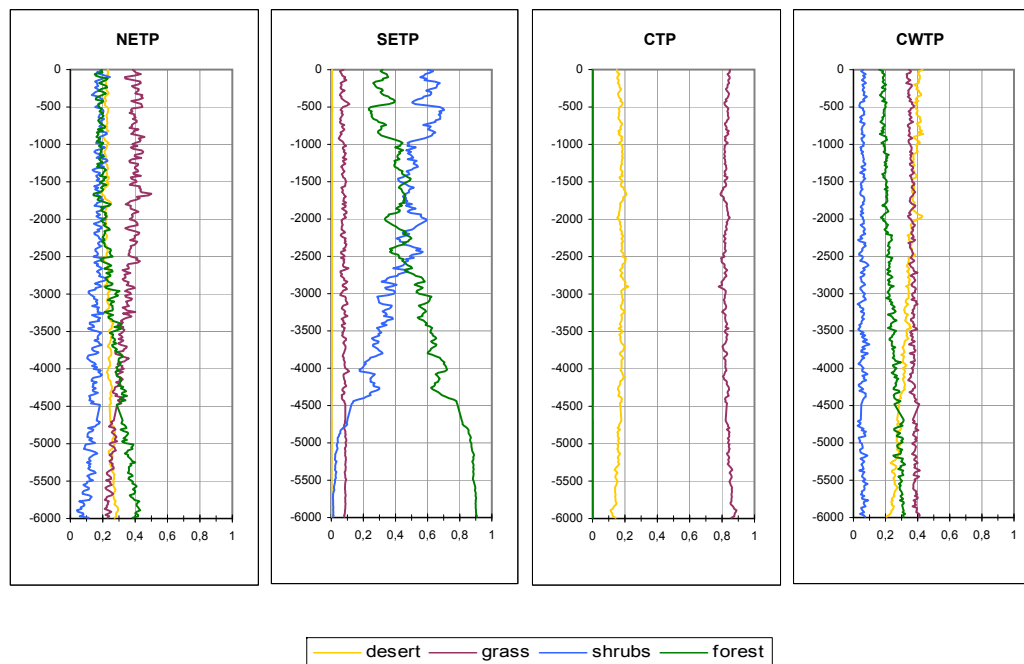


Fig. 4. Simulated vegetation trend (20 yr-mean) from mid-Holocene 6000 years before present to present-day, averaged for 4 different regions on the Tibetan Plateau: the north-eastern Tibetan Plateau (NETP), the south-eastern Tibetan Plateau (SETP), the central Tibetan Plateau (CTP) and the central-western Tibetan Plateau (CWTP), see Fig. 2. Values are given in fraction per grid box.

[Title Page](#)[Abstract](#)[Introduction](#)[Conclusions](#)[References](#)[Tables](#)[Figures](#)[⏪](#)[⏩](#)[◀](#)[▶](#)[Back](#)[Close](#)[Full Screen / Esc](#)[Printer-friendly Version](#)[Interactive Discussion](#)

Holocene vegetation and biomass changes on the Tibetan Plateau

A. Dallmeyer et al.

Title Page

Abstract

Introduction

Conclusions

References

Tables

Figures

◀

▶

◀

▶

Back

Close

Full Screen / Esc

Printer-friendly Version

Interactive Discussion

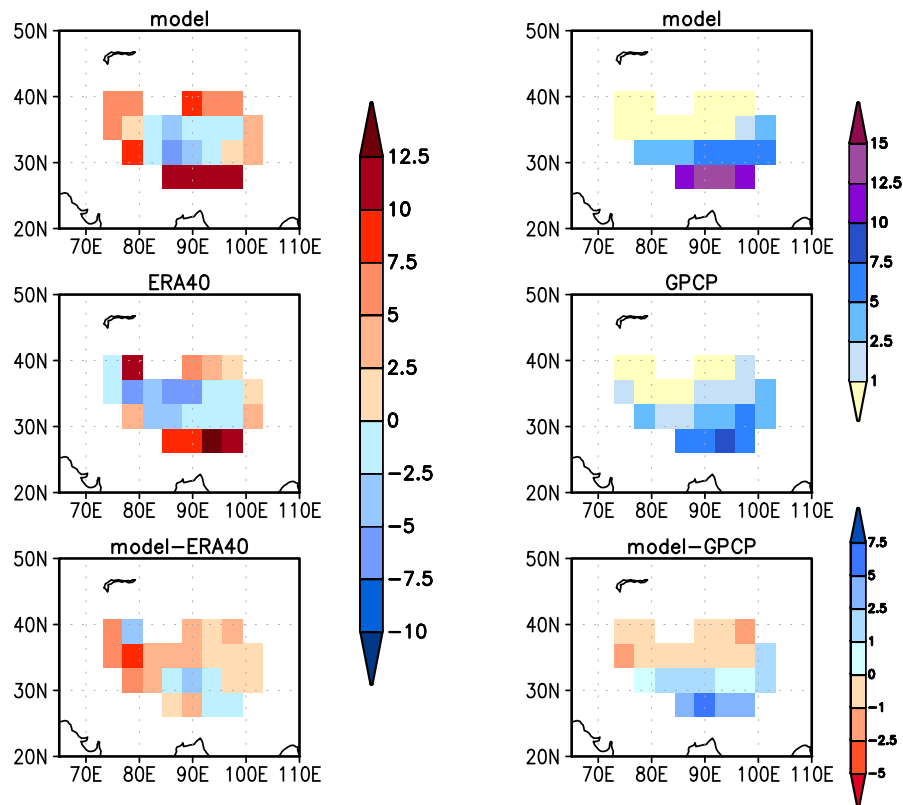


Fig. 5. Annual mean 2m-temperature in °C (left panel) and summer precipitation in mm day⁻¹ (right panel) calculated from the last 100 years of our coupled model experiment and a reference dataset. For temperature, results are compared with the reanalysis data ERA40 (Simmons and Gibson, 2000); for precipitation, observational data GPCP (Adler et al., 2003) is used. Shown are also differences between model results and the reference dataset.

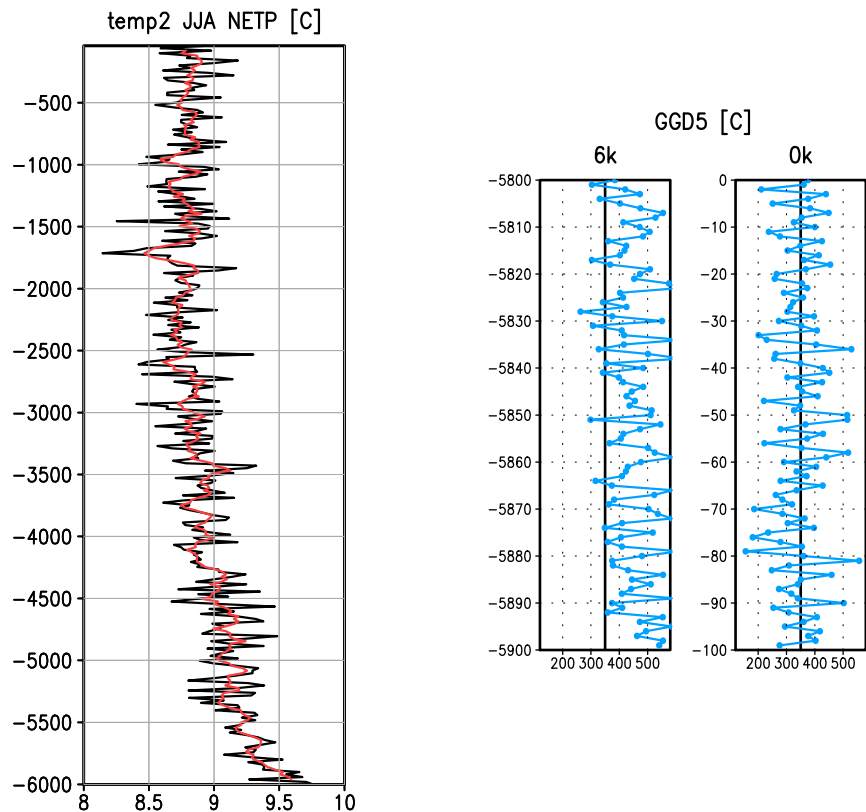


Fig. 6. Change of the climate factors yielding the land cover change on the north-eastern Tibetan Plateau (NETP), left panel: 20-yr-mean summer near-surface air temperature trend ($^{\circ}\text{C}$) from mid-Holocene (-6000 years) to present-day. The red solid line shows the 100-yr-running-mean. Right panel: difference in growing degree days between 100 years of mid-Holocene (-5900 years to -5800 years) and the last 100 years of the simulation period representing present-day. The solid black line marks the GDD5 threshold for extratropical forest of 350°C .

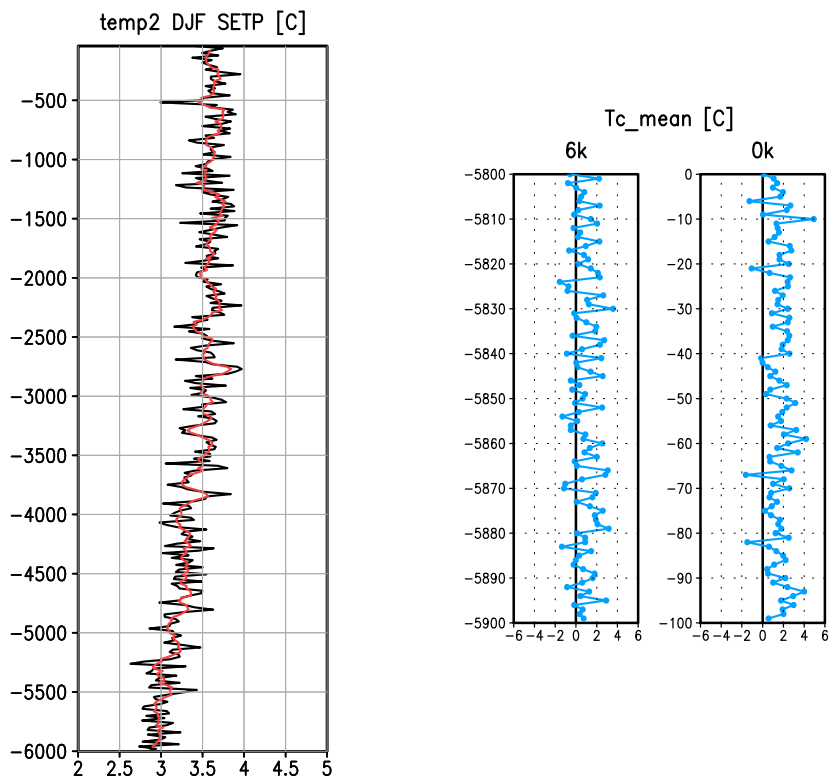


Fig. 7. Change of the climate factors yielding the land cover change on the south-eastern Tibetan Plateau (SETP), left panel: 20-yr-mean winter near-surface air temperature trend ($^{\circ}\text{C}$) from mid-Holocene (-6000 years) to present-day. Red solid line shows the 100-yr-running-mean. Right panel: difference in mean near-surface air-temperature of the coldest month between 100 years of mid-Holocene (-5900 years to -5800 years) and the last 100 years of the simulation period representing present-day. Raingreen shrubs are limited by frost events; the solid black line marks the freezing point (0°C).

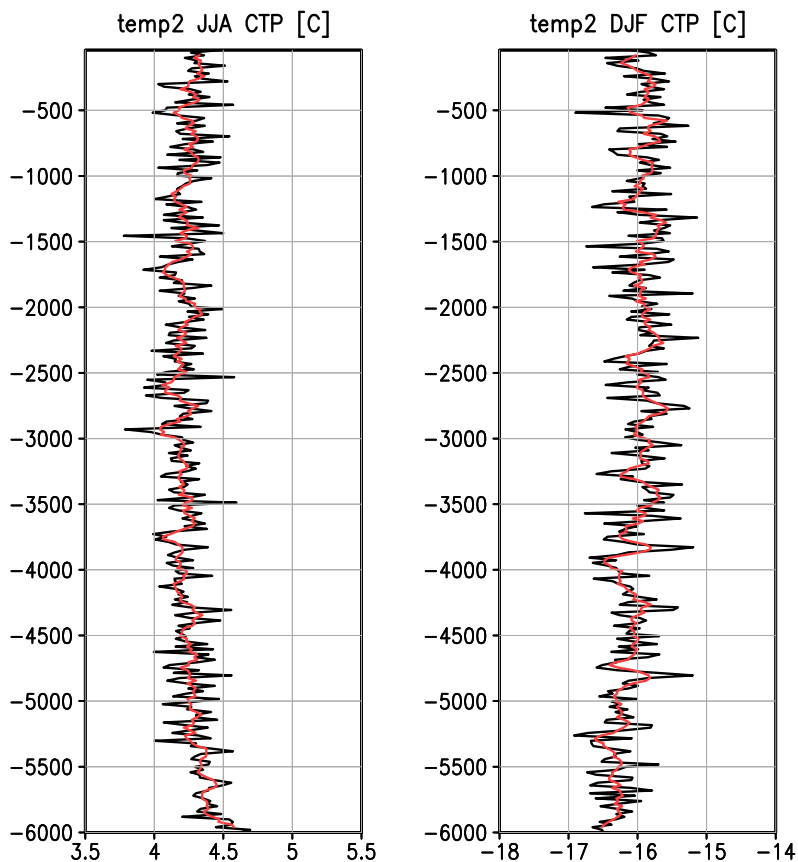


Fig. 8. Simulated change of summer (JJA) and winter (DJF) 20 yr-mean near-surface air temperature ($^{\circ}\text{C}$) for the last 6000 years on the central Tibetan Plateau (CTP). The red solid line shows the 100 yr-running-mean.

Holocene vegetation and biomass changes on the Tibetan Plateau

A. Dallmeyer et al.

Title Page

Abstract

Introduction

Conclusions

References

Tables

Figures

◀

▶

◀

▶

Back

Close

Full Screen / Esc

Printer-friendly Version

Interactive Discussion

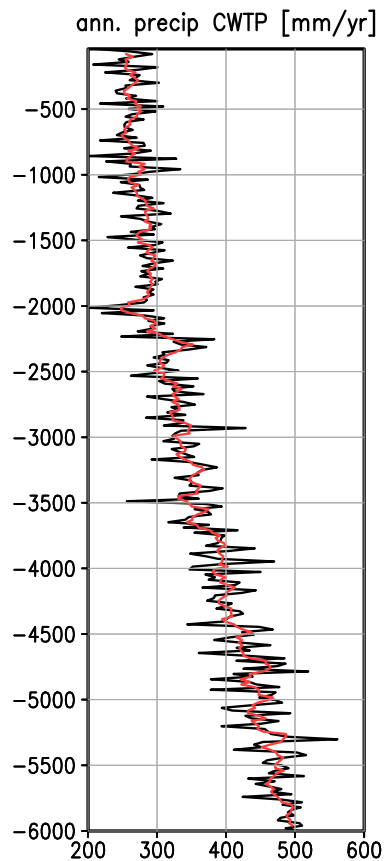


Fig. 9. Simulated change of 20 yr-mean annual precipitation (mm yr^{-1}) for the last 6000 years on the central-western Tibetan Plateau (CWTP). The red solid line shows the 100 yr-running mean.

Holocene vegetation and biomass changes on the Tibetan Plateau

A. Dallmeyer et al.

Title Page

Abstract

Introduction

Conclusions

References

Tables

Figures

◀

▶

◀

▶

Back

Close

Full Screen / Esc

Printer-friendly Version

Interactive Discussion